

Electronic Supplementary Information (ESI) for Chem. Commun.

Highly Dispersed Pt Anchored on Hollow Carbon Nanobowls: Negative Curvature Boosts Electrocatalytic Hydrogen Evolution

Yuxing Ma,^a Rong Hua,^a Youfeng Pan,^a Xin Li,^a Mengxue Ma,^a Mengying Wang,^a Haifen Ding,^a Haoquan Zheng^{a,b*}

^aKey Laboratory of Applied Surface and Colloid Chemistry, Ministry of Education, School of Chemistry and Chemical Engineering, Shaanxi Normal University, Xi'an 710119, China.

^bShanghai Key Laboratory of High-resolution Electron Microscopy, ShanghaiTech University, Shanghai 201210, China.

Correspondence Email: zhenghaoquan@snnu.edu.cn

1. Experimental section

1.1 Materials

Tetraethyl orthosilicate (TEOS) was purchased from Energy Chemical. Nafion (5 wt %) was obtained from Shanghai Hesen Electric Co. Ltd. Other reagents were purchased from Sinopharm Chemical Reagent Co. Ltd. (Shanghai, China). All reagents were used as received.

1.2 Synthesis of HCB.

The precursor solution was prepared by mixing ammonia (10 ml), ethanol (70 ml) and deionized water (30 ml), and then rapidly stirring for 5 min. Tetraethyl orthosilicate (TEOS, 5 mL) was added dropwise under continuous stirring for 1 h. Subsequently, resorcinol (0.4 g) and formaldehyde (0.6 mL) were introduced, and the reaction proceeded for 24 h at room temperature. The obtained intermediates were purified through repeated washing with ethanol/water and dried at 65 °C. Carbonization was performed at 850 °C for 2 h under N₂ flow, followed by silica removal using 10 wt% HF solution.

1.3 Synthesis of HCS.

The HCS material was prepared following the same protocol, with modified reagent quantities: TEOS (3 mL), resorcinol (0.8 g), and formaldehyde (1.2 mL).

1.4 Synthesis of HCB@Pt.

Initially, 20 mg of HCB material was dispersed in 10 ml of 1-butyl-3-methylimidazolium hexafluorophosphate (C₈H₁₅N₂F₆P) (M_w = 284.19). To this suspension, 10 mg of H₂PtCl₆·6H₂O was added along with an appropriate amount of H₂O/ethanol, followed by ultrasonication for 1 h. The resulting complex was collected by centrifugation. The precipitate was then dispersed into 1 mg aqueous solution and reduced with slightly excess sodium borohydride (NaBH₄) to obtain the final HCB@Pt catalyst (with a molar ratio of approximately 1:1 to the Pt precursor).

1.5 Synthesis of HCS@Pt.

HCS@Pt was prepared using an identical procedure, with HCS replacing HCB as the

supporting material.

1.6 Characterization

Scanning electron microscopy (SEM, Hitachi SU8020) at an accelerating voltage of 5 kV and transmission electron microscope (TEM, JEOL JEM-2100) with a field emission gun operating at 200 kV were used to observe the morphology of the samples. EDS analysis was conducted on an AMETEK Materials Analysis EDX equipped on the TEM. Infrared spectra were collected by the Brüker TENSOR 27 instrument. Powder X-ray diffraction (PXRD) patterns of the materials were conducted on an X-ray diffractometer (Bruker, D8 Advance, Cu $K\alpha$, $\lambda = 1.5406 \text{ \AA}$, 40 kV/40 mA). Micromeritics ASAP 2020 was used to measure the Brunauer-Emmett-Teller (BET) specific surface area of the materials. The Raman spectrometer (Renishaw, in Via Reflex) and X-ray photoelectron spectroscopic (XPS) spectra were carried out to analyze the structural composition, valence state, and bonding state of the materials. Inductively coupled plasma mass spectrometry (ICP-MS) was performed on NexION 2000 ICP-MS instrument (PerkinElmer) to quantitatively analyze the amount of attached guest metal ions.

1.7 Electrochemical measurement

All the relevant HER tests were carried out on the CHI 660E (CH Instruments) electrochemical workstation. In this experiment, Ag/AgCl was used as the reference electrode and graphite as the opposite electrode. The potentials in this experiment were converted to a reversible hydrogen electrode (RHE) ($E_{\text{RHE}} = E_{\text{Ag/AgCl}} + 0.197 + 0.0591 \times \text{pH}$). In detail, the homogeneous catalyst ink was prepared by mixing 2 mg of catalyst, 333 μL of deionized water, 166 μL of ethanol, and 10 μL of Nafion solution, then ultrasonically for 1 h. Drop 6 μL of catalyst ink on the surface of the glassy carbon (GC) (3 mm, 0.07 cm^2) as the working electrode. LSV testing was measured in 0.5 M H_2SO_4 (pH = 0.26) with a scan rate of 5 $\text{mV} \cdot \text{s}^{-1}$ after 100% IR compensation.

1.8 Measurement of electrochemically active surface area

The electrochemically active surface area (ECSA) was determined using the double-layer capacitance method. Constant potential cyclic voltammetry (CV) scans were performed in the double-layer region, ranging from 0.5 to 0.6 V vs RHE, with scan rates of 10, 20, 30, 40, 50, 60, 70, 80, 90, and 100 $\text{mV} \cdot \text{s}^{-1}$. Taking the current (i)

corresponding to the potential point in the middle of these CV curves as the Y-axis and the scanning rate (v) as the X-axis, the function graph of i and v is plotted. The slope of the obtained straight line is the C_{dl} value. There is a positive correlation between ECSA and C_{dl} value (C_s is the specific capacitance of the catalyst sample), from which the ECSA of the material can be estimated:

$$i = vC_{dl}$$
$$\text{ECSA} = \frac{C_{dl}}{C_s}$$

1.9 Membrane electrode assembly (MEA)

The Proton exchange membrane water electrolysis (PEMWE) cell was assembled with 1 cm² flow field plates containing a catalyst-loaded gas diffusion electrode (GDE, ~ 0.25 mg cm⁻²) as the cathode and an IrO₂-coated titanium mesh as the anode. The catalyst ink was prepared by ultrasonically dispersing 5 mg of catalyst in a mixture of 950 μ L ethanol and 50 μ L Nafion solution (5 wt%). The MEA was fabricated by hot-pressing the catalyst-coated carbon paper and IrO₂/Ti mesh onto opposite sides of a Nafion 117 membrane. All electrochemical measurements were conducted at 50 °C with electrolyte circulation at 15 mL min⁻¹, where polarization curves were obtained under steady-state conditions and system stability was evaluated through chronoamperometric i - t testing at a constant potential of 1.66 V.

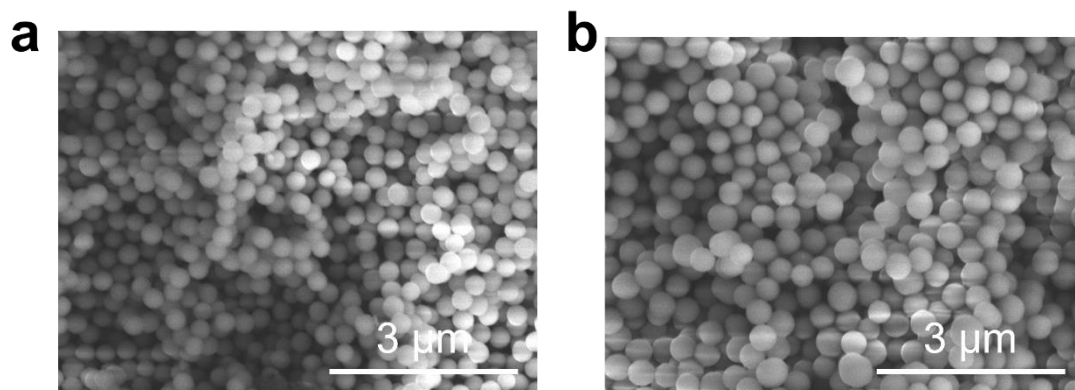


Fig. S1. SEM images showing SiO₂-RF hybrid morphologies: (a) HCB and (b) HCS.

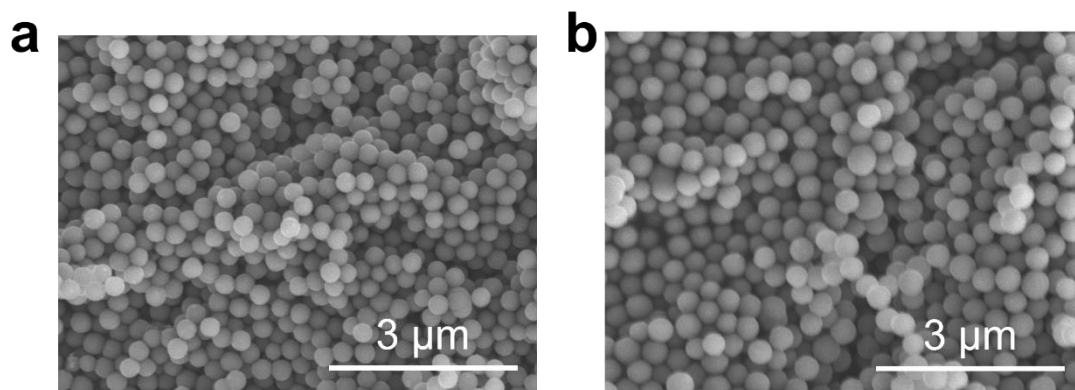


Fig. S2. SEM images showing SiO₂-C hybrid morphologies: (a) HCB and (b) HCS.

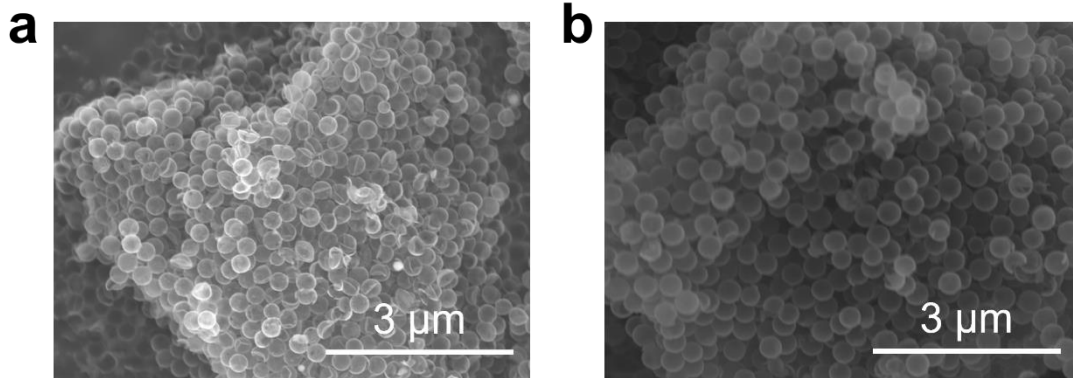


Fig. S3. SEM images of (a) HCS and (b) HCB.

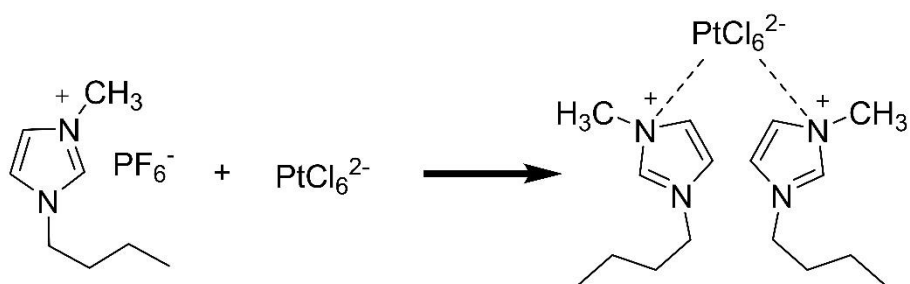


Fig. S4. The reaction process between $\text{C}_8\text{H}_{15}\text{N}_2\text{F}_6\text{P}$ and H_2PtCl_6 .

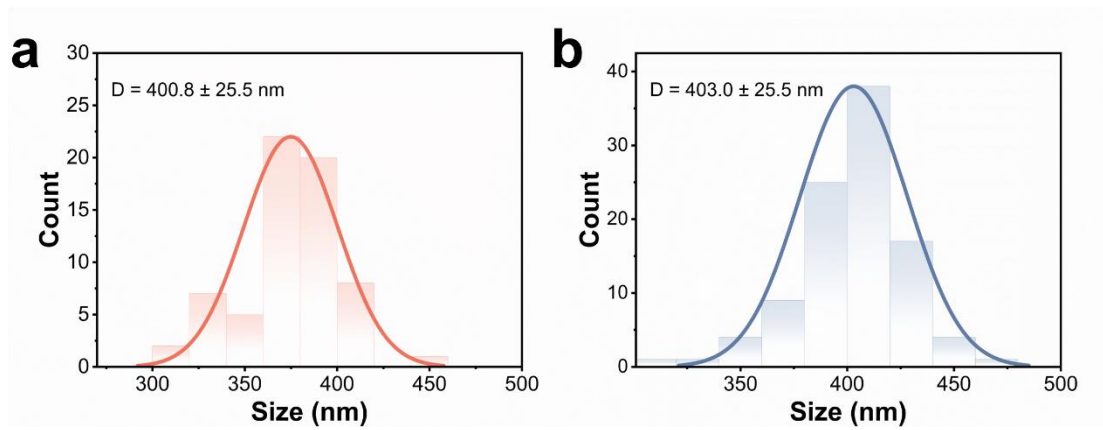


Fig. S5. Particle size distributions of (a) HCB and (b) HCS.

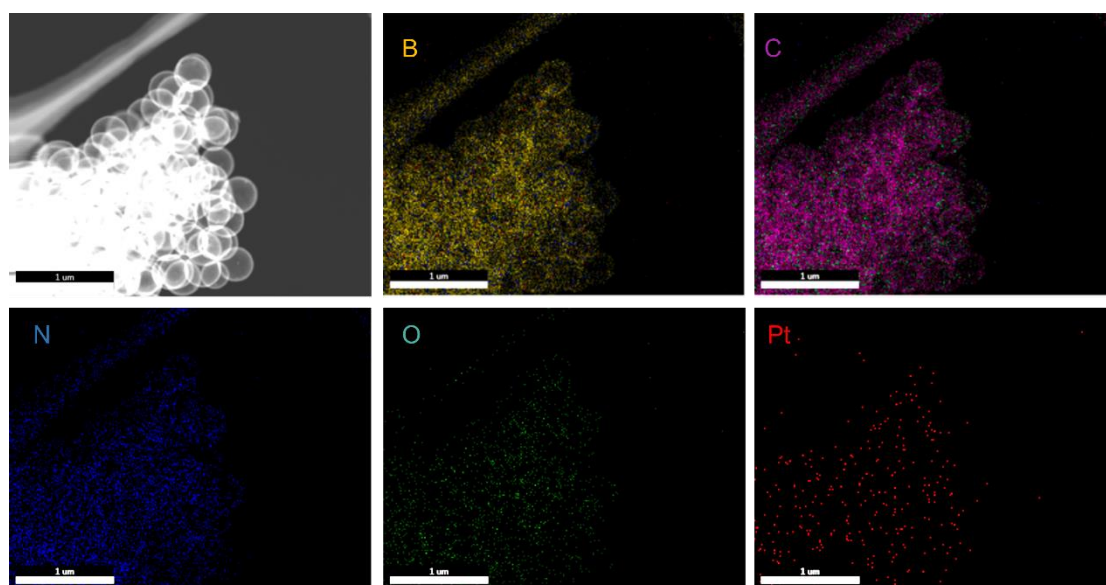


Fig. S6. Elemental mapping images of HCS@Pt.

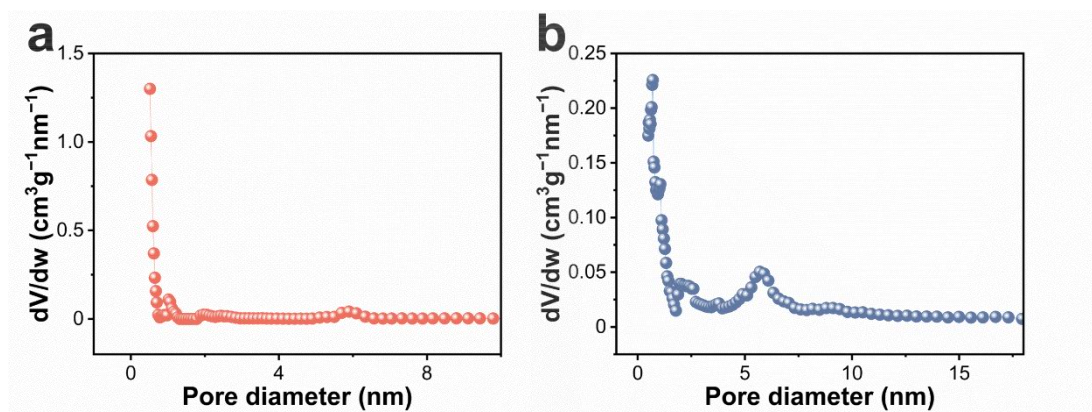


Fig. S7. Pore size distribution curves of (a) HCB@Pt and (b) HCS@Pt.

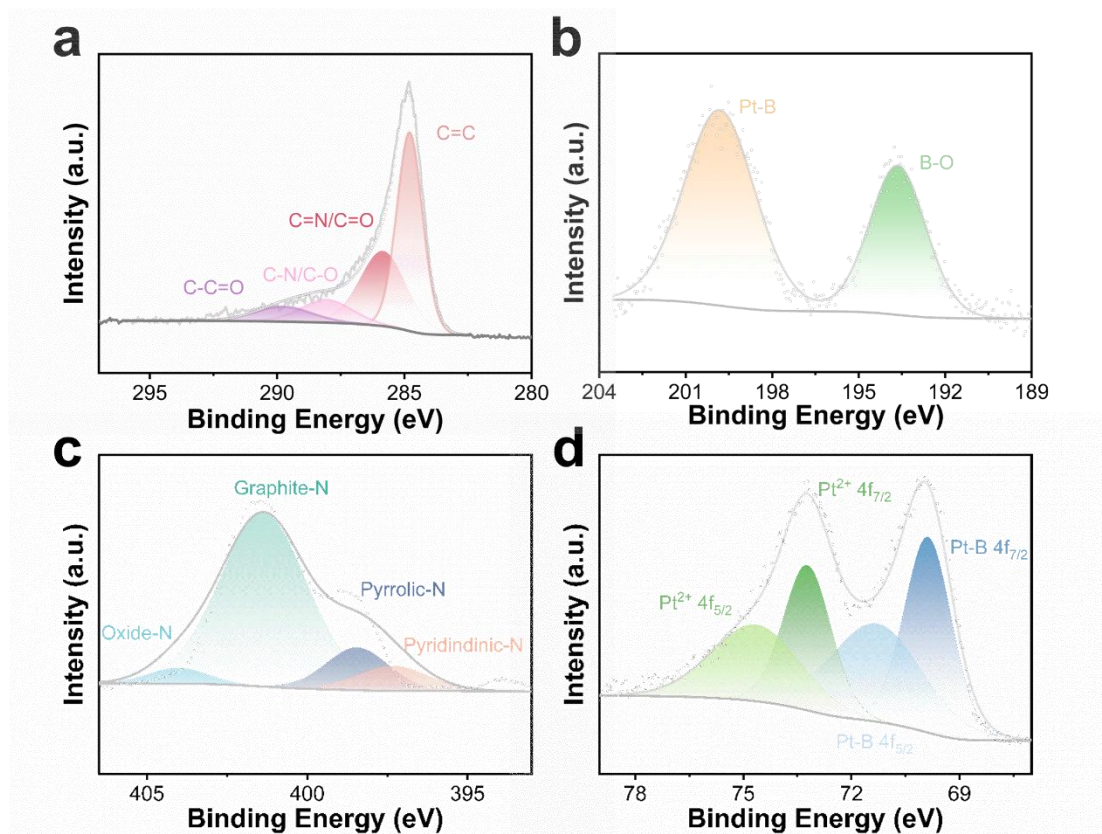


Fig. S8. High-resolution XPS spectra of HCB@Pt: (a) C 1s, (b) B 1s, (c) N 1s and (d) Pt 4f.

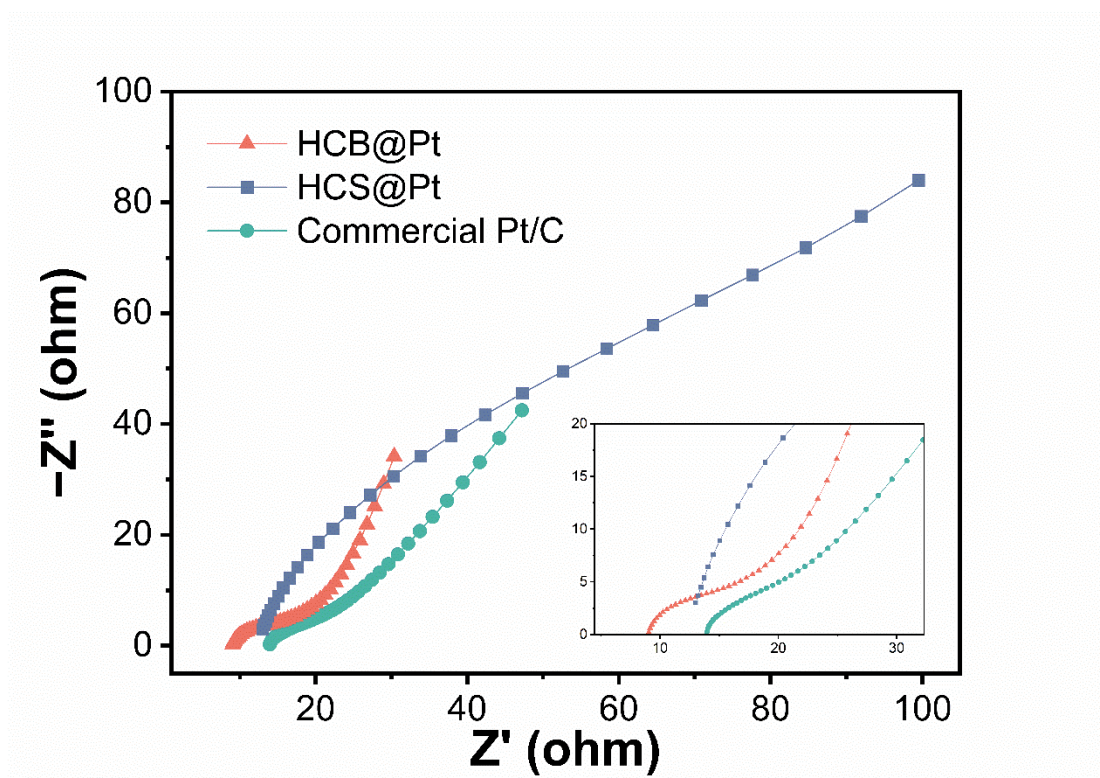


Fig. S9. Nyquist plots for HCB@Pt, HCS@Pt and commercial Pt/C.

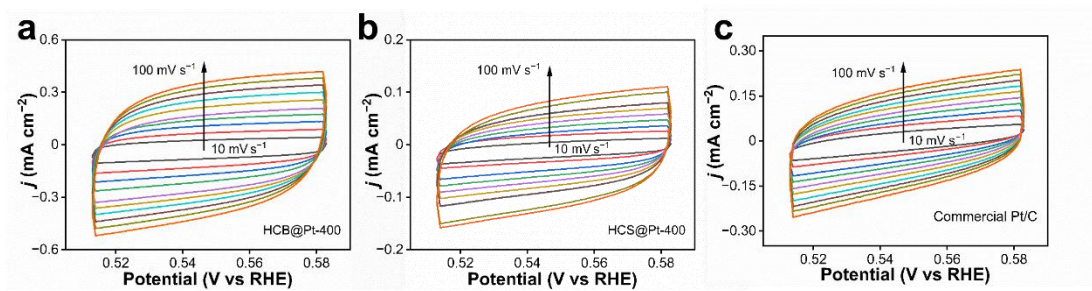


Fig. S10. CV curves of catalysts at different sweep speeds: (a) HCB@Pt, (b) HCS@Pt and (c) Commercial Pt/C in 0.5 M H_2SO_4 .

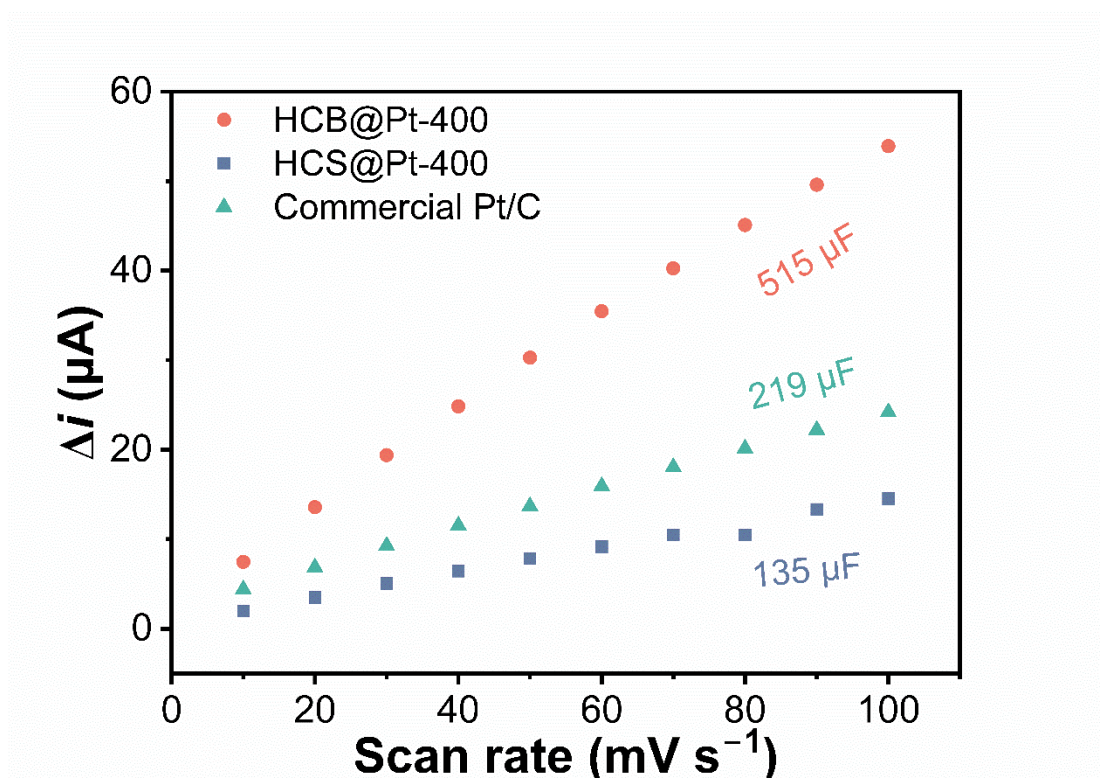


Fig. S11. C_{dl} images derived from the CV curves.

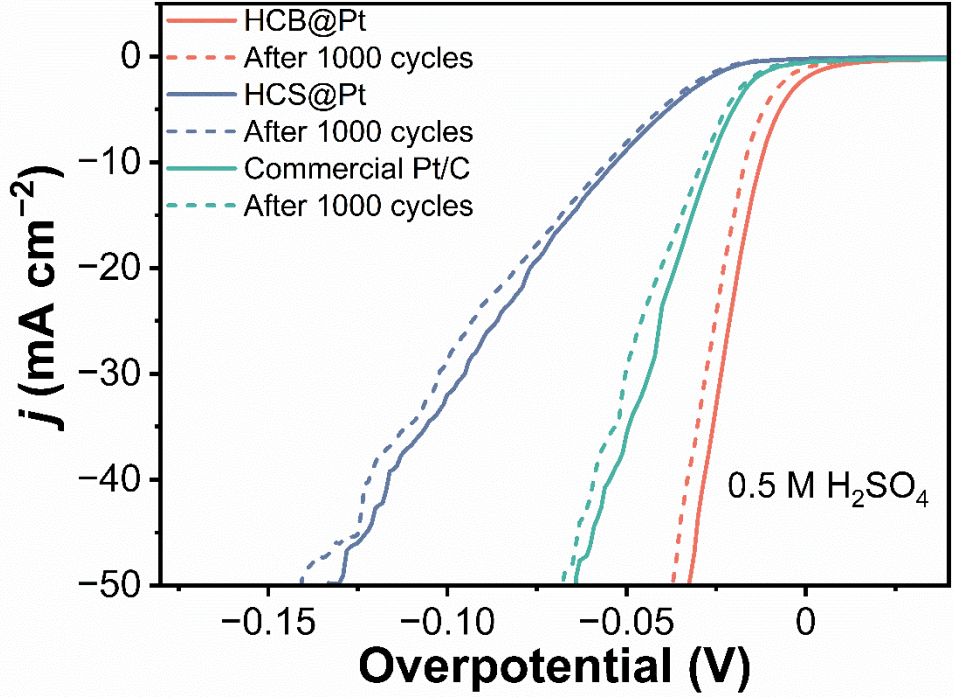


Fig. S12. Comparison of LSV curves for HCB@Pt, HCS@Pt, and commercial Pt/C before and after 1000 CV cycles.

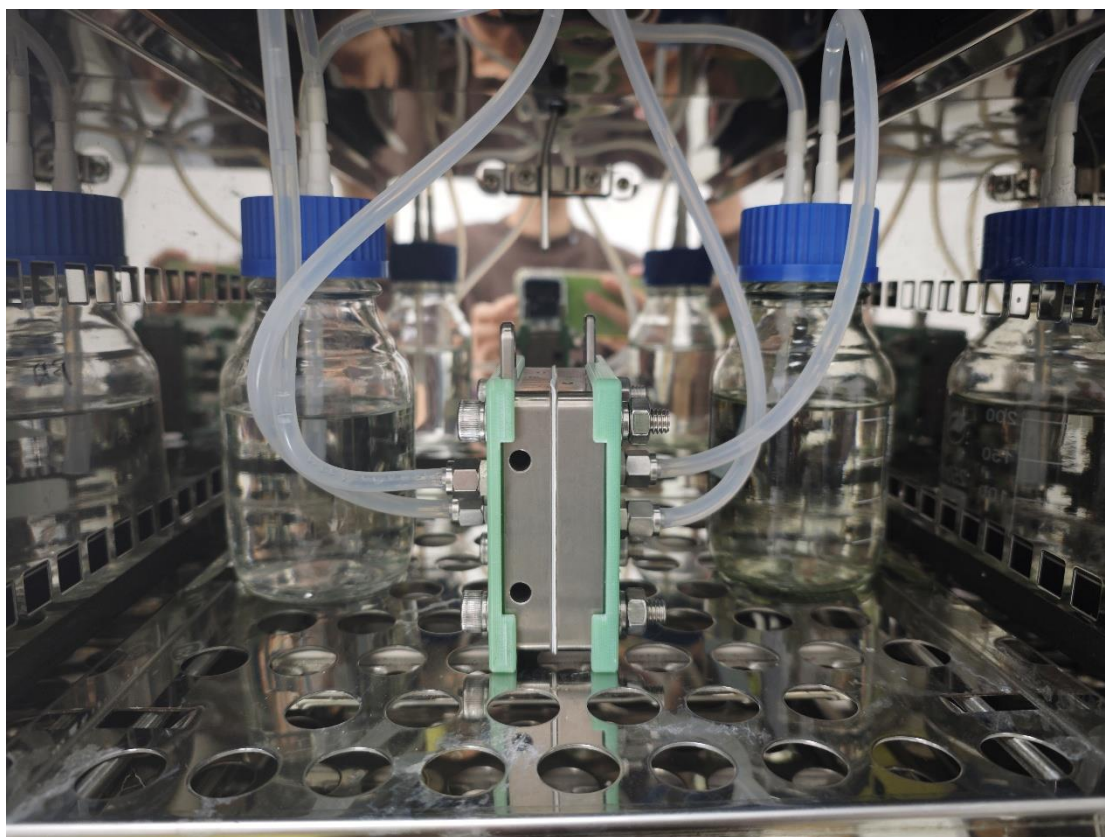


Fig. S13. Photo of the PEMWE cell.

Table S1. Surface elemental composition (at%) derived from XPS analysis.

Sample	B (at%)	C(at%)	N (at%)	O (%)
HCB@Pt	0.39	82.08	2.81	14.72
HCS@Pt	1.91	82.69	2.48	12.92

Table S2. Comparison of overpotentials and Tafel plots for recently reported noble metal catalysts under acidic conditions.

Catalysts	Over potential (mV)	Tafel (mV dec ⁻¹)	<i>j</i> (mA cm ⁻²)	Ref.
HCB@Pt	11	24.7	10	This work
HCB@Pt	31	/	50	This work
Ru-MoO _{3-x} /Mo ₂ AlB ₂	38	57.1	10	1
NC@RuSA-CoP	15.6	48.1	10	2
Pt-Ru/CNT	12	23	10	3
Pt/OLC	38	35	10	4
Pt@C ₂ N	~ 40	33	10	5
Pt-MoS ₂	~ 145	96	10	6
p-CN@S-Pt&Ni B	40.6	29.26	10	7
p-CN@S-Pt&Ni B	67	/	25	7
Pt ₃ V@Pt	13	17.4	10	8
PtSe ₂ /PtCo	38	22	10	9
Pt@PtIr NDs	22	14.6	10	10
Pt NDs	26	15.7	10	10
Pt NPs@CF	35	28	10	11

Table S3. Comparison of Pt loading between our work and other reports in PEMWE.

Catalysts	Potential	PEM	Temperature	Ref.
HCB@Pt	1.45 V@10 mA cm⁻²	N117	50 °C	This work
HCB@Pt	1.66 V@200 mA cm⁻²	N117	50 °C	This work
HCB@Pt	1.76 V@400 mA cm⁻²	N117	50 °C	This work
Pt/Mo ₂ C-L/Mo	1.55 V@10 mA cm ⁻²	/	/	12
Pt/Mo ₂ C-L/Mo	1.8 V@122 mA cm ⁻²	/	/	12
20 wt% Pt/C	2.1 V@247 mA cm ⁻²	N117	60 °C	13
Pt-NCS-2	2.1 V@435 mA cm ⁻²	N117	60 °C	13
PANI/Ni ₂ P	1.82 V@1000 mA cm ⁻²	N117	80 °C	14
Alloyed Pt SA	~1.75 V@500 mA cm ⁻²	N117	80 °C	15
Alloyed Pt SA	1.82 V@1000 mA cm ⁻²	N117	80 °C	15
Pt VN	~1.82 V@500 mA cm ⁻²	N117	80 °C	15
D-PtCu/CF	1.63 V@500 mA cm ⁻²	/	60 °C	16

References:

- 1 Y. Yang, D. Pang, C. Wang, Z. Fu, N. Liu, J. Liu, H. Wu, B. Jia, Z. Guo, X. Fan and J. Zheng, *Angew. Chem., Int. Ed.*, 2025, **n/a**, e202504084.
- 2 Z. Wang, K. Chi, S. Yang, J. Xiao, F. Xiao, X. Zhao and S. Wang, *Small*, 2023, **19**, 2301403.
- 3 D. Zhang, Z. Wang, X. Wu, Y. Shi, N. Nie, H. Zhao, H. Miao, X. Chen, S. Li, J. Lai and L. Wang, *Small*, 2022, **18**, 2104559.
- 4 D. Liu, X. Li, S. Chen, H. Yan, C. Wang, C. Wu, Y. A. Haleem, S. Duan, J. Lu, B. Ge, P. M. Ajayan, Y. Luo, J. Jiang and L. Song, *Nat. Energy*, 2019, **4**, 512-518.
- 5 J. Mahmood, F. Li, S.-M. Jung, M. S. Okyay, I. Ahmad, S.-J. Kim, N. Park, H. Y. Jeong and J.-B. Baek, *Nat. Nanotechnol.*, 2017, **12**, 441-446.
- 6 J. Deng, H. Li, J. Xiao, Y. Tu, D. Deng, H. Yang, H. Tian, J. Li, P. Ren and X. Bao, *Energy Environ. Sci.*, 2015, **8**, 1594-1601.
- 7 Y. Zuo, T. Li, N. Zhang, T. Jing, D. Rao, P. Schmuki, Š. Kment, R. Zbořil and Y. Chai, *ACS Nano*, 2021, **15**, 7790-7798.
- 8 Z. Zhong, Y. Tu, L. Zhang, J. Ke, C. Zhong, W. Tan, L. Wang, J. Zhang, H. Song, L. Du and Z. Cui, *ACS Catal.*, 2024, **14**, 2917-2923.
- 9 B. Hao, M. Gan, J. Guo, G. Li, Y. Song, Y. Shen, B. Xu, P. Liu and J. Guo, *Adv. Funct. Mater.*, 2025, **35**, 2413916.
- 10 C. Liu, Z. Wei, M. Cao and R. Cao, *Nano Res.*, 2024, **17**, 4844-4849.
- 11 Q. Li, Z. Deng, D. Tao, J. Pan, W. Xu, Z. Zhang, H. Zhong, Y. Gao, Q. Shang, Y. Ni, X. Li, Y. Chen and Q. Zhang, *Adv. Funct. Mater.*, 2024, **34**, 2411283.
- 12 H. Yuan, L. Zhao, B. Chang, Y. Chen, T. Dong, J. He, D. Jiang, W. Yu, H. Liu and W. Zhou, *Appl. Catal., B*, 2022, **314**, 121455.
- 13 B. Jiang, H. Yuan, Q. Dang, T. Wang, T. Pang, Y. Cheng, K. Wu, X. Wu and M. Shao, *Int. J. Hydrogen Energy*, 2019, **44**, 31121-31128.
- 14 H. Shi, J. Qian and X. Hu, *J. Power Sources*, 2024, **596**, 234099.
- 15 H. Gao, Y. Jiang, R. Chen, C.-L. Dong, Y.-C. Huang, M. Ma, Z. Shi, J. Liu, Z. Zhang, M. Qiu, T. Wu, J. Wang, Y. Jiang, J. Chen, X. An, Y. He and S. Wang, *Adv. Funct. Mater.*, 2023, **33**, 2214795.
- 16 M. Zhou, Y. Zhao, X. Zhao, P.-F. Yin, C.-K. Dong, H. Liu, X.-W. Du and J. Yang, *ACS Appl. Energy Mater.*, 2024, **7**, 3848-3857.